Research Article
Cancer

JOURNAL
OF HEPATOLOGY

Genomic sequencing identifies WNK2 as a driver in hepatocellular carcinoma and a risk factor for early recurrence

Graphical abstract

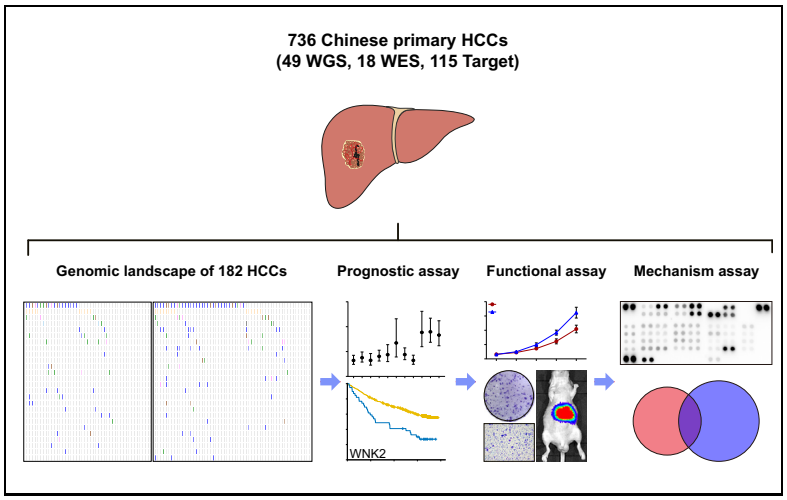

Highlights

- 182 Chinese hepatocellular carcinomas were sequenced.
- *WNK2*, *RUNX1T1*, *CTNNB1*, *TSC1*, and *TP53* somatic mutations correlated with early tumor recurrence after curative resection.
- WNK2 displayed somatic mutation, copy number loss, and downregulated expression in HCC.
- WNK2 deficiency leads to ERK1/2 signalling activation, TAM infiltration, and tumor growth and metastasis.

Authors

Shao-Lai Zhou, Zheng-Jun Zhou, Zhi-Qiang Hu, ..., Ya Cao, Jia Fan, Jian Zhou

Correspondence

zhou.jian@zs-hospital.sh.cn
(J. Zhou)

Lay summary

We applied next-generation sequencing and conducted an in-depth genomic analysis of hepatocellular carcinomas from a Chinese patient cohort. The results delineate the genomic events that characterize hepatocellular carcinomas in Chinese patients and identify *WNK2* as a driver associated with early tumor recurrence after curative resection.

http://dx.doi.org/10.1016/j.jhep.2019.07.014
 J. Hepatol. 2019, 71, 1152–1163

Research Article
Cancer

JOURNAL OF HEPATOLOGY

Genomic sequencing identifies WNK2 as a driver in hepatocellular carcinoma and a risk factor for early recurrence

Shao-Lai Zhou[1,2,†], Zheng-Jun Zhou[1,2,†], Zhi-Qiang Hu[1,†], Cheng-Li Song[3,†], Yi-Jie Luo[3], Chu-Bin Luo[1], Hao-Yang Xin[1], Xin-Rong Yang[1], Ying-Hong Shi[1], Zheng Wang[1], Xiao-Wu Huang[1,4], Ya Cao[6], Jia Fan[1,2,4,5], Jian Zhou[1,2,4,5,*]

[1]*Department of Liver Surgery and Transplantation, Liver Cancer Institute, Zhongshan Hospital, Fudan University; Key Laboratory of Carcinogenesis and Cancer Invasion (Fudan University), Ministry of Education, Shanghai 200032, China;* [2]*Institute of Biomedical Sciences, Fudan University, Shanghai 200032, China;* [3]*Novogene Bioinformatics Institute, Beijing 100083, China;* [4]*Shanghai Key Laboratory of Organ Transplantation, Zhongshan Hospital, Fudan University, Shanghai 200032, China;* [5]*State Key Laboratory of Genetic Engineering, Fudan University, Shanghai 200032, China;* [6]*Cancer Research Institute, Central South University; Key Laboratory of Carcinogenesis and Cancer Invasion, Ministry of Education, Changsha 410078, China*

Background & Aims: Early recurrence of hepatocellular carcinoma (HCC) after curative resection is common. However, the association between genetic mechanisms and early HCC recurrence, especially in Chinese patients, remains largely unknown.
Methods: We performed whole-genome sequencing (49 cases), whole-exome sequencing (18 cases), and deep targeted sequencing (115 cases) on 182 primary HCC samples. Focusing on *WNK2*, we used Sanger sequencing and qPCR to evaluate all the coding exons and copy numbers of that gene in an additional 554 HCC samples. We also explored the functional effect and mechanism of WNK2 on tumor growth and metastasis.
Results: We identified 5 genes (*WNK2*, *RUNX1T1*, *CTNNB1*, *TSC1*, and *TP53*) harboring somatic mutations that correlated with early tumor recurrence after curative resection in 182 primary HCC samples. Focusing on *WNK2*, the overall somatic mutation and copy number loss occurred in 5.3% (39/736) and 27.2% (200/736), respectively, of the total 736 HCC samples. Both types of variation were associated with lower WNK2 protein levels, higher rates of early tumor recurrence, and shorter overall survival. Biofunctional investigations revealed a tumor-suppressor role of WNK2: its inactivation led to ERK1/2 signaling activation in HCC cells, tumor-associated macrophage infiltration, and tumor growth and metastasis.
Conclusions: Our results delineate genomic events that characterize Chinese HCCs and identify *WNK2* as a driver of early HCC recurrence after curative resection.
Lay summary: We applied next-generation sequencing and conducted an in-depth genomic analysis of hepatocellular carcinomas from a Chinese patient cohort. The results delineate the genomic events that characterize hepatocellular carcinomas in Chinese patients and identify *WNK2* as a driver associated with early tumor recurrence after curative resection.

Introduction

Hepatocellular carcinoma (HCC) is a relatively common type of cancer with rising incidence and mortality rate.[1] Approximately half of the 782,500 new cases of liver cancer and the 745,500 deaths due to liver cancer that occur worldwide each year occur in China.[1] In China, most HCCs arise from hepatitis B,[2] other risk factors such as exposures to aflatoxin[3] and aristolochic acids[4] can also be important in HCC development. Those etiological factors may result in different genetic alterations, as well as different therapeutic targets, in Chinese patients compared with patients from other countries and regions.

Over the past decade, new discoveries have shed light on the molecular basis of HCC pathogenesis. Following technological advances, several pioneering studies have delineated the genetic landscape underlying liver carcinogenesis,[5–11] including amplifications on chromosomes 6p21 (*VEGFA*) and 11q13 (*FGF19*/*CNND1*) and deletions on chromosome 9 (*CDKN2A*). Mutations in the coding regions of *TP53* and *CTNNB1* affect 25–30% of patients with HCC and, along with low-frequency mutations in some other genes (*e.g.*, *AXIN1*, *ARID2*, *ARID1A*, *TSC1*/*TSC2*), define core pathways that are commonly deregulated in HCC. Many genomic changes related to HCC have been characterized in Western and Japanese populations; however, the genomic landscape of HCC in the Chinese population has only been investigated in small patient cohorts, either with specified aflatoxin-associated HCC[3] or with low sequencing depth.[9] To gain a comprehensive understanding of the molecular etiology of HCC, it is essential that we learn more about the genomic changes associated with HCC in the Chinese population.

Advances in the treatment and management of patients with HCC have improved survival rates; however, HCC still has a high

Keywords: Hepatocellular Carcinoma; Early Recurrence; Sequencing; WNK2.
Received 30 January 2019; received in revised form 21 June 2019; accepted 3 July 2019; available online 23 July 2019
* Corresponding author. Address: Liver Cancer Institute, Zhongshan Hospital, Fudan University, 136 Yi Xue Yuan Road, Shanghai 200032, China. Tel.: +86 21 64041990, fax: +86 21 64037181.
E-mail address: zhou.jian@zs-hospital.sh.cn (J. Zhou).
† These authors contributed equally to this work.

rate of early recurrence, which limits long-term survival even after surgical resection.[12–14] Although several studies have revealed biomarkers that shed light on the molecular mechanisms underlying HCC progression and prognosis,[15] the association between genetic mechanisms and early HCC recurrence, especially in Chinese patients, remains largely unknown.

We aimed to systematically define genomic alterations in Chinese patients with HCC and to identify mutations associated with early tumor recurrence in those patients. We performed whole-genome sequencing (WGS) of 49 matched pairs of tumor and normal tissues and whole-exome sequencing (WES) of 18 similarly matched pairs from patients with HCC who had tumor early tumor recurrence after curative resection. We next selected 97 genes and performed very deep, targeted sequencing of 115 additional HCC samples and paired normal tissues (34 from patients that experienced early recurrence and 81 from patients that did not experience early recurrence). Using all 182 HCC samples, we compared the frequency of somatic mutations in specific genes between the patients that experienced early recurrence and those that did not experience early recurrence. Then, focusing on *WNK2*, we used Sanger sequencing and qPCR to evaluate all of the coding exons and copy numbers of that gene in an additional 554 HCC samples and paired normal tissues (117 from patients that experienced early recurrence and 437 from patients that did not experience early recurrence) to investigate its value in predicting early tumor recurrence and overall survival (OS). Finally, we explored the functional effect and mechanism of WNK2 on tumor growth and metastasis.

Materials and methods

Detailed information about the patients and follow-up; DNA preparation, DNA capture, and sequencing; WGS, WES and targeted sequencing; date quality control; reads mapping and detection of somatic genetic alterations; spectrum and signatures of somatic mutations; significantly mutated genes; Sanger sequencing; inferring HBV/AAV2 genotype and identification of integration; cell lines, animals, and lentiviral vector; cell proliferation, colony formation, and matrigel invasion assays; *in vivo* assays for tumor growth and metastasis; RNA isolation, quantitative reverse transcription PCR, and RT^{2}profiler PCR array; western blot and phosphokinase array analysis; TMA and immunohistochemistry; evaluation of immunohistochemical variables and statistical analysis are available in the CTAT table and supplementary methods.

Results

Overview of genomic alterations in patients with primary HCC who had early tumor recurrence

To discover the genomic alterations in Chinese patients with HCC who had early tumor recurrence after curative resection, we performed WGS of tumor and matched non-cancerous liver-tissue samples from 49 patients with HCC (all of whom had early tumor recurrence after curative resection). The average sequencing depth was 54.5-fold for tumors and 36.1-fold for normal tissues (Table S2). We mapped the sequence reads to the human reference genome and identified a total of 1,662,031 somatic single-nucleotide variants (SNVs) and 36,684 indels, with 2,446–99,031 mutations per tumor genome (Table S3-5). Sanger sequencing to validate 1,146 randomly selected somatic coding mutations showed a high true-discovery rate (95.5%), with an average of 6.52 (range = 0.82–33.01) somatic mutations per Mb (Fig. 1A). We classified 7 tumor samples (14.3% of the samples) with mutation rates of >10/Mb as hypermutated.[16]

C>A transversions and C>T and T>C transitions were ubiquitous in all of the HCCs (Fig. 1B), a feature shared by other HCC cohorts.[5–7,17] Of the 7 hypermutated HCCs, 6 also had a dominant T>A transversion pattern, however, and the remaining hypermutated HCC had a dominant C>G transversion pattern, implying that those substitutions might contribute to hypermutation in HCC. The T>A transversion pattern was significantly associated with the total number of somatic SNVs among all the HCC samples (Fig. S2A), which further suggested that the T>A transversion contributes to somatic SNVs in Chinese patients with HCC.

Mutation signature analysis of 96 substitution patterns[17,18] identified 5 signatures in the HCC samples (Signatures A–E; Fig. 1C-D, Fig. S3, Table S6). Signature A was characterized by dominant T>A mutations and was highly similar to the previously described Signature 22 (cosine correlation similarity = 0.98), which is known to result from exposure to aristolochic acid and to be associated with a high mutational burden.[4] Consistent with that, Signature A was a predominant signature in the hypermutated HCC samples and was significantly associated with the total number of somatic SNVs among all 49 HCC samples (Fig. S2B). Signature B, characterized by C>G mutations, was only dominant in 1 sample, which was also the sample with the highest number of SNVs across all 49 HCCs. Signature B had low cosine correlation similarity to the previously described Signature 13. Therefore, it represents a new mutational signature. Signature C, characterized by C>A mutations, showed a strong similarity to the previously described Signature 24 (correlation similarity = 0.92), which has been associated with exposure to aflatoxin in cancers. Signatures D and E were mainly characterized by C>T and T>C mutations and showed similarity to the previously described Signature 5 (correlation similarity = 0.84) and Signature 16 (correlation similarity = 0.91), which have been revealed to be associated with aging and alcohol consumption, respectively.[7,19,20]

We identified 32 amplified segments, which harbored several known oncogenes such as *CCND1*, *TERT*, and *MYC*. We also identified 18 lost segments, which harbored tumor suppressors including *TP53* (17p13), *RB1* (13q14), and *CDKN2A* (9q21) (Fig. 1E, Fig. S4, Table S7). Additionally, we detected abundant genomic structural variations (SVs), with a mean of 43.4 SVs (range = 0–224) per sample. The SVs comprised 483 deletions, 18 deletions with inversion, 189 deletions with insertion, 414 tandem duplications, 3 insertions, and 1,019 intra- or inter-chromosomal translocations (Fig. 1F, Table S8). We found that HBV integration occurred in 26 (53%) of the tumor samples. We identified recurrent HBV integration events at *TERT* - a well-known HCC driver gene. We also identified HBV insertions upstream of *CCNE1* in a tumor sample, which were associated with aggressive tumor behavior (Table S9).

Identification of *WNK2, RUNX1T1, CTNNB1, TSC1, and TP53* somatic mutations associated with early HCC recurrence after curative resection

We performed WES of 18 pairs of tumor and matched normal tissues (average sequencing depth: 113.7-fold for tumors and 110.9-fold for normal tissues; Tables S2, S10) and combined

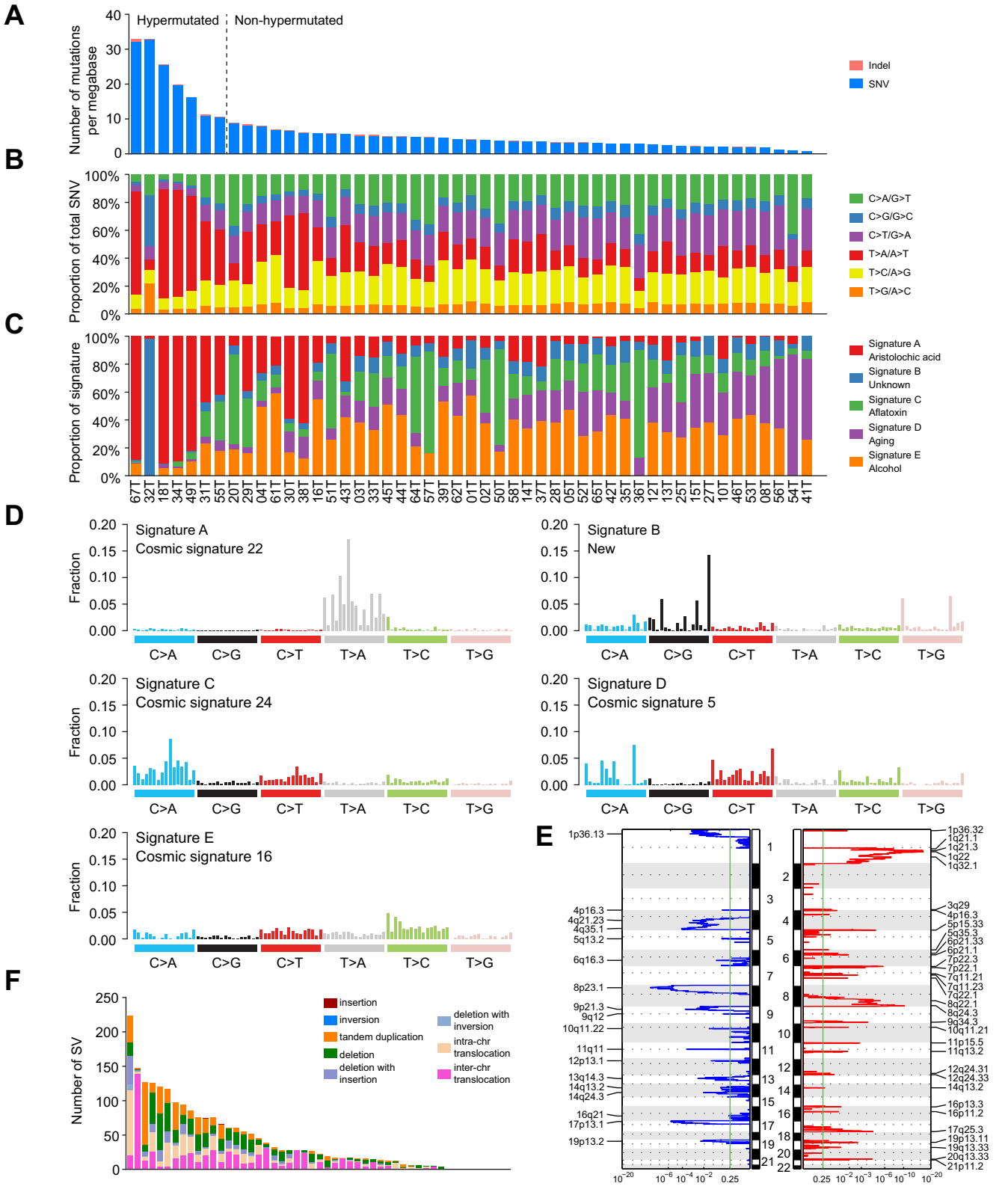

Fig. 1. Global genomic alterations in 49 Chinese primary HCCs that had early tumor recurrence. (A) Mutational burden in the whole genome across 49 HCCs. Seven cases with mutation rates of >10/Mb (14.3% of all cases) were classified as hypermutated. (B) Distribution of 6 substitution patterns sorted by the total mutation number. (C) Proportion of signatures observed in each HCC sample. (D) Patterns of 5 signatures (Signatures A, B, C, D and E) identified in 49 HCC genomes; the most similar COSMIC signature to each is also indicated. (E) GISTIC analysis revealed the whole-genome distribution of copy number alterations. GISTIC q-values (x-axis) for deletions (left, blue) and amplifications (right, red) are plotted across the genome (y-axis). (F) The number of structural variations in 49 HCCs, including insertions, inversions, tandem duplications, deletions, inter-, and intra-chromosomal translocations.

the somatic SNVs and indels identified in the protein-coding exons with the data obtained from WGS. We identified 10 significantly mutated genes using MutSigCV, 6 of which (*TP53*, *AXIN1*, *CTNNB1*, *CDKN1A*, *ALB,* and *ARID1A*) were identified as potential cancer drivers in previous studies (Table S11). We then designed a gene panel consisting of all exon regions of 97 genes and the *TERT* promoter (Table S12). The genes in the panel fell into the following categories: i) 7 significantly mutated genes identified by MutSigCV (excluding *KRTAP5-6*, *SLC10A2*, and *HIST1H2BD* because of their low mutation frequency and lack of known relation to tumor development or progression) and several other genes that were frequently mutated in our samples, ii) genes that were previously documented as components of a cancer-related pathway or as potential therapeutic targets, and iii) previously reported HCC driver genes.[5–7] We performed very deep, targeted sequencing of an additional 115 samples of HCC tumors and paired normal tissues. The average sequencing depth was 2,149.6-fold for the tumors and 2,239.9-fold for the normal tissues (Tables S2, S13).

Using the next-generation sequencing results from the total set of 182 HCC samples, we compared the frequency of somatic mutations in specific genes between the HCCs from patients that experienced early recurrence and those that did not experience early recurrence. We found that *WNK2* had the most significant difference in mutation frequency: *WNK2* was mutated in 12 of 101 HCC samples (11.9%) from patients that experienced early recurrence but only 1 of 81 HCC samples from patients that did not experience early recurrence ($p = 0.006$). Some other genes, such as *RUNX1T1* ($p = 0.018$), *CTNNB1* ($p = 0.019$), and *TSC1* ($p = 0.044$), also had a significant

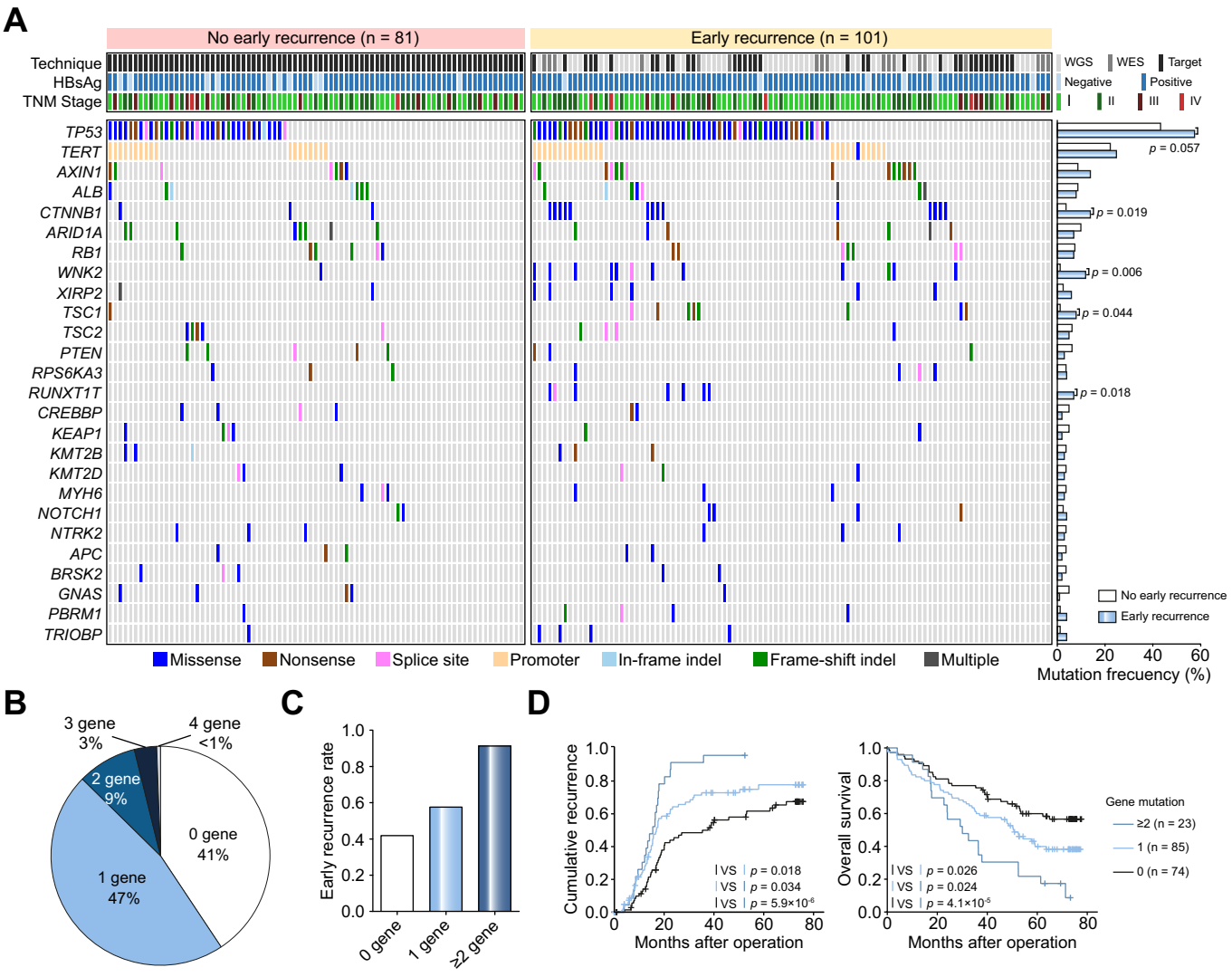

Fig. 2. Gene mutations associated with early tumor recurrence after curative resection in 182 primary HCCs. (A) The mutational spectrum in HCCs with or without early recurrence, identified through whole-genome sequencing, whole-exome sequencing, or targeted sequencing. Genes present in ≥5 samples are shown. All mutations were validated by Sanger sequencing. The chi-square or Fisher's exact tests were used. (B) Proportions of 182 HCCs carrying *WNK2*, *RUNX1T1*, *CTNNB1*, *TSC1*, and *TP53* mutations. (C) Early recurrence rates in patients with HCC carrying different numbers of mutated genes (*WNK2*, *RUNX1T1*, *CTNNB1*, *TSC1*, and *TP53*). (D) Kaplan-Meier survival analysis showing cumulative recurrence rates and overall survival rates based on *WNK2*, *RUNX1T1*, *CTNNB1*, *TSC1*, and *TP53* mutations. Log-rank test was used.

difference in mutation frequency between the 2 groups of patients, while *TP53* had a marginal difference ($p = 0.057$) between the groups (Fig. 2A, genes present in ≥5 samples are shown).

When we looked at the combination of those 5 genes (*WNK2*, *RUNX1T1*, *CTNNB1*, *TSC1*, and *TP53*), we found that 21 of 23 patients (91.3%) with mutations in 2 or more of those genes, 49 of 85 patients (57.6%) with a mutation in only 1 of those genes, and 31 of 74 patients (49.1%) with no mutations in those genes experienced early recurrence (Fig. 2B-C). Furthermore, the 5-year cumulative recurrence rate was highest (95.7%) in the patients with mutations in 2 or more of the 5 genes, which was significantly higher than the rate in the patients with a mutation in only 1 of the genes (72.6%) and in those with no mutations in the 5 genes (57.6%). Similarly, the 5-year OS rate among the patients with mutations in 2 or more of the genes was 30.4%, which was significantly lower than that among the patients with a mutation in only 1 of the genes (53.9%) and in none of the genes (67.3%; Fig. 2D).

Somatic mutations, copy number loss, and reduced expression of *WNK2* were predictive of early tumor recurrence after curative resection

We evaluated all the coding exons of *WNK2* in an additional 554 HCC samples and paired normal tissues by Sanger sequencing. We found *WNK2* somatic mutations in 17 of 117 HCCs from patients that experienced early recurrence and in 9 of 437 HCCs from patients that did not experience early recurrence.

Overall, from the total set of 736 HCC cases included in our study, we identified 40 *WNK2* somatic mutations in 39 different patients: 29 of the 218 patients (13.3%) that experienced early recurrence and 10 of the 518 patients (1.9%) that did not experience early recurrence (Fig. 3A-B, Fig. S5). Polyphen-2 analysis revealed that most of those mutations were predicted to adversely affect the function of the WNK2 protein (Table S14).

WNK2 is located within a large genomic region of chromosome 9q (chr9:34399801–141213431) that was recurrently deleted in our initial set of 49 WGS HCC samples (Fig. 1E, Table S7). We performed qPCR to assess the copy number of *WNK2* in all 736 HCC cases. The results showed that *WNK2* copy number loss occurred in 27.2% (200/736, calculated copy number: 0.13–0.99) of the samples (Fig. 3C).

We further evaluated WNK2 expression by immunohistochemistry in all 736 HCCs. The results showed that WNK2 expression was downregulated in tumor samples compared with that in adjacent non-tumor liver samples (Fig. 3D-E). The patients with *WNK2* somatic mutation or copy number loss showed a further decrease in tumor WNK2 expression level (Fig. 3E).

We then correlated *WNK2* somatic mutation, copy number loss, and expression level with the patients' clinical characteristics and outcomes. Somatic mutations in *WNK2* were correlated with increased tumor size, vascular invasion, and satellite lesions. *WNK2* copy number loss was correlated with increased tumor size, increased tumor number, vascular invasion, satellite lesions, and increased tumor differentiation and TNM stage. The WNK2 expression level was correlated with a higher gamma-glutamyltransferase level, increased tumor size and tumor number, vascular invasion, satellite lesions, and increased TNM stage (Table S15).

Among the 736 patients with HCC, those with *WNK2* somatic mutation, copy number loss, or reduced expression exhibited an elevated rate of early recurrence (Fig. 3F). Although some clinical characteristics such as tumor size and satellite lesions are predictive of early tumor recurrence after curative resection, patients with *WNK2* somatic mutation, copy number loss, or lower expression were more likely than patients without those features to experience early tumor recurrence (Fig. 3G). Kaplan-Meier survival analysis also revealed significantly shorter OS and higher cumulative recurrence rates for patients with *WNK2* somatic mutation, copy number loss, or lower expression compared with patients without those features (Fig. 3H). Univariate and multivariate analyses confirmed that *WNK2* somatic mutation, copy number loss, and lower expression were independent prognostic factors for OS and time to recurrence (Table S16).

WNK2 functions as a tumor-suppressor gene in HCC

Our results suggested a possible tumor-suppressor role for *WNK2* in HCC. To test that hypothesis, we analyzed the genotype and expression of *WNK2* in 6 HCC cell lines. All 6 HCC cell lines were validated as wild-type (WT) by Sanger sequencing, using the same filter criteria as used for the HCC samples in next-generation sequencing. qPCR showed that high metastatic HCC cell lines: MHCC97L, MHCC97H, and HCCLM3 had *WNK2* copy number loss (Fig. 4A). Western blots confirmed that WNK2 protein levels in 6 established HCC cell lines were decreased in comparison to the non-transformed hepatic cell line L0-2, especially in those HCC cell lines with high metastatic potential (MHCC97L, MHCC97H, and HCCLM3; Fig. 4A).

Next, we knocked down *WNK2* in HepG2 and Hep3B cells. Biofunctional investigations revealed that the knockdown of *WNK2* resulted in an increase in HCC cell proliferation and colony formation activity (Fig. 4B-C, Fig. S6B-C) and led to enhanced invasive ability (Fig. 4D, Fig. S6D). *In vivo* HCC mouse models showed that *WNK2* knockdown accelerated tumor growth and pulmonary metastasis (Fig. 4E, Fig. S6E).

We generated lentiviral constructs to re-express *WNK2* in HCCLM3 and MHCC97H cells. For *WNK2* mutants, mutation sites located in protein kinase domain or oxidative-stress-responsive kinase 1 C-terminal domain, as well as some other sites that were recurrently mutated in our HCC samples, were selected. The results showed that overexpression of WT *WNK2* substantially suppressed HCC cell proliferation, colony formation, and invasion ability. In contrast, the mutated *WNK2* failed to cause those effects, in whole or in part (Fig. 4B-D, Fig. S6B-D). In agreement with the *in vitro* studies, analysis of an *in vivo* HCC mouse model showed that WT *WNK2* significantly suppressed tumor growth and pulmonary metastasis, while the mutated *WNK2* yielded a larger tumor volume and increased pulmonary metastasis compared with the WT *WNK2* (Fig. 4E, Fig. S6E). Interestingly, we found that the nonsense mutant $WNK2^{K211X}$ and the frameshift mutant $WNK2^{T275fs}$ lost nearly all of their suppressive effects on HCC cells, which suggested that truncating mutations in the protein kinase domain destroyed the function of WNK2. These results support the notion that *WNK2* is a tumor-suppressor gene in HCC and that certain somatic mutations abolish its function and its tumor-inhibitory effect.

WNK2 inactivation leads to ERK1/2 signaling activation in HCC cells

We investigated the mechanism of WNK2 function in HCC cells using a phosphokinase array and HCC cells with altered WNK2 expression. The results showed that p-ERK1/2 were upregulated

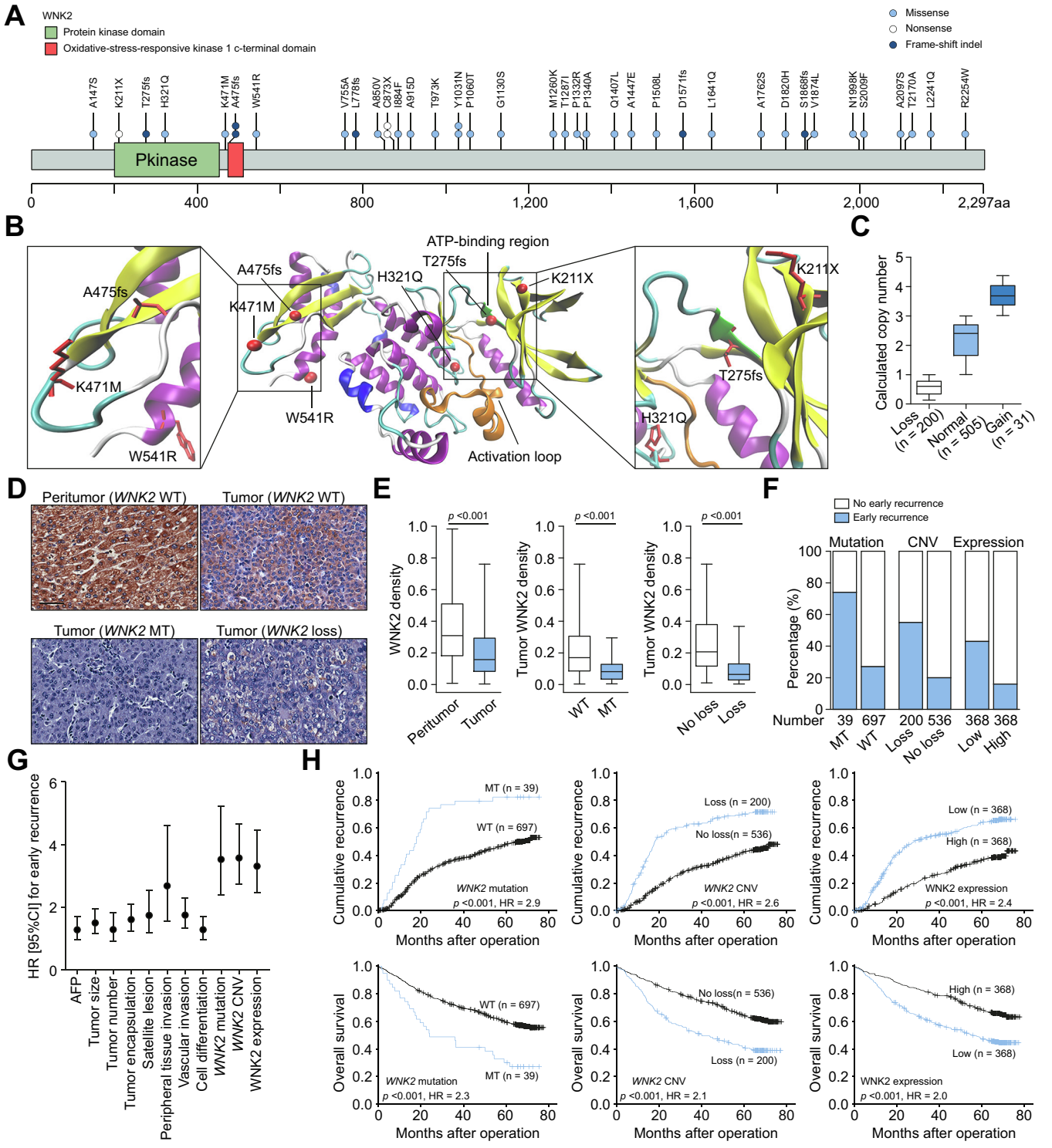

Fig. 3. Clinical significance of WNK2 alteration in 736 HCCs. (A) Distribution of the somatic mutations in *WNK2* identified in this study. (B) Structural homology model of WNK2 kinase and oxidative-stress-responsive kinase 1 C-terminal domain based on the crystal structure of WNK3 (PDB, 5o2c), on which are mapped the residues that are altered in HCC. All numbering of amino acids is based on the WNK2 protein sequences. Mutant residues are shown as red spheres and sticks models (ATP binding site and activation loop are shown as green and orange, respectively). (C) Calculated *WNK2* copy numbers identified in 736 HCCs. (D) Representative WNK2 staining in peritumor tissues and tumor tissues with wild-type *WNK2*, mutant *WNK2* (K211X), and *WNK2* loss; scale bars = 50 μm. (E) The statistics of WNK2 staining density in different groups. Student's *t* test was used. (F) Early recurrence rates in patients with HCC with mutant or wild-type *WNK2*, copy number loss or no loss of *WNK2*, and low or high WNK2 expression. (G) The ability of *WNK2* mutation, copy number variation, and expression level to predict early recurrence compared with that of other clinical parameters. (H) Kaplan-Meier survival analysis showing cumulative recurrence rates and overall survival rates based on *WNK2* mutation, copy number variation, and expression level. Log-rank test was used.

by more than 100% in HepG2 cells after knockdown of *WNK2*, whereas they were downregulated by more than 50% in HCCLM3 cells following WNK2 overexpression (Fig. 5A). Western blot analysis validated these results and showed that compared with WT *WNK2*, mutated *WNK2* failed to suppress ERK1/2 signaling, which suggests that WNK2 negatively modulates

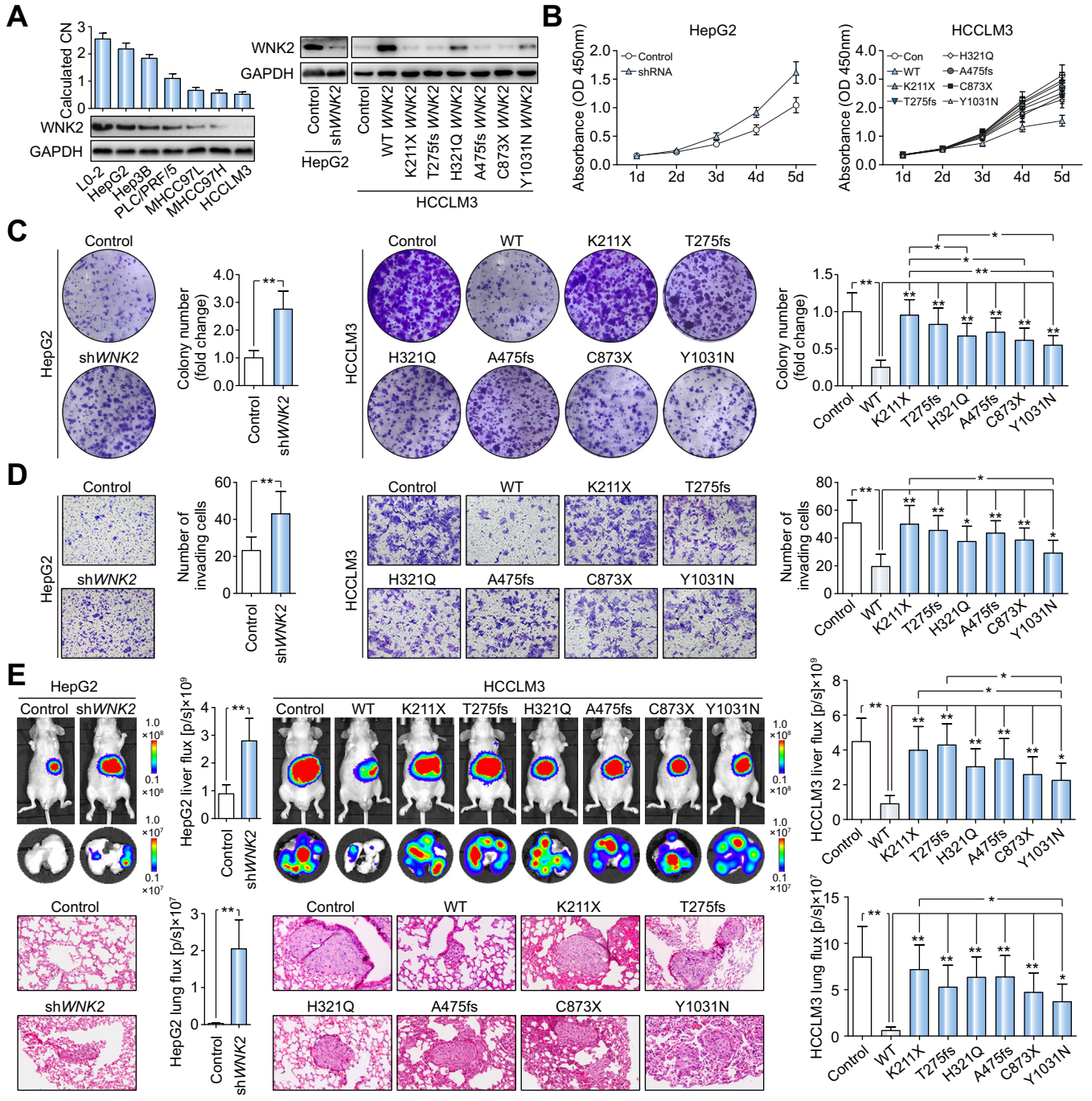

Fig. 4. Identification of *WNK2* as a tumor-suppressor gene in HCC. (A) *WNK2* copy number revealed by qPCR in 1 normal liver cell line (L0-2) and 6 HCC cell lines, and WNK2 expression examined by western blot in parent and stably transfected cells. (B) Proliferation of HepG2 cells after *WNK2* knockdown and of HCCLM3 cells expressing wild-type or mutant *WNK2* compared with that of controls. (C) Colony formation activity of HepG2 cells after *WNK2* knockdown and of HCCLM3 cells expressing wild-type or mutant *WNK2* compared with that of controls. The bar graphs illustrate the quantification of the colony formation assay, $^{*}p$ <0.05, $^{**}p$ <0.01. Student's *t* test was used. (D) Cell invasion of HepG2 cells after *WNK2* knockdown and of HCCLM3 cells expressing wild-type or mutant *WNK2* compared with that of controls. The graphs depict the number of invasive cells after 48 h, $^{*}p$ <0.05, $^{**}p$ <0.01. Student's *t* test was used. (E) Representative bioluminescence images of mouse liver tumors and pulmonary metastasis, and H&E stained images of metastatic nodules in lungs. The color scale bar depicts the photon flux emitted from the mice, $^{*}p$ <0.05, $^{**}p$ <0.01. Student's *t* test was used.

ERK1/2 signaling and that its mutation or downregulation activates that signaling pathway in HCC cells (Fig. 5B). Immunohistochemistry staining exhibited concordant results in tumor sections from HCC cell-derived mouse models (Fig. 5C). Clinical HCC samples with *WNK2* somatic mutation or copy number loss tended to have strong p-ERK1/2 expression, as revealed by immunohistochemistry staining (Fig. 5D), which further indicated that *WNK2* inactivation activates ERK1/2 signaling in HCC. Furthermore, U0126 (an MEK1/2 inhibitor) treatment significantly alleviated the increased cell proliferation, colony formation, and invasion *in vitro* (Fig. 5E-G) and the increased tumor growth and pulmonary metastasis *in vivo* (Fig. 5H)

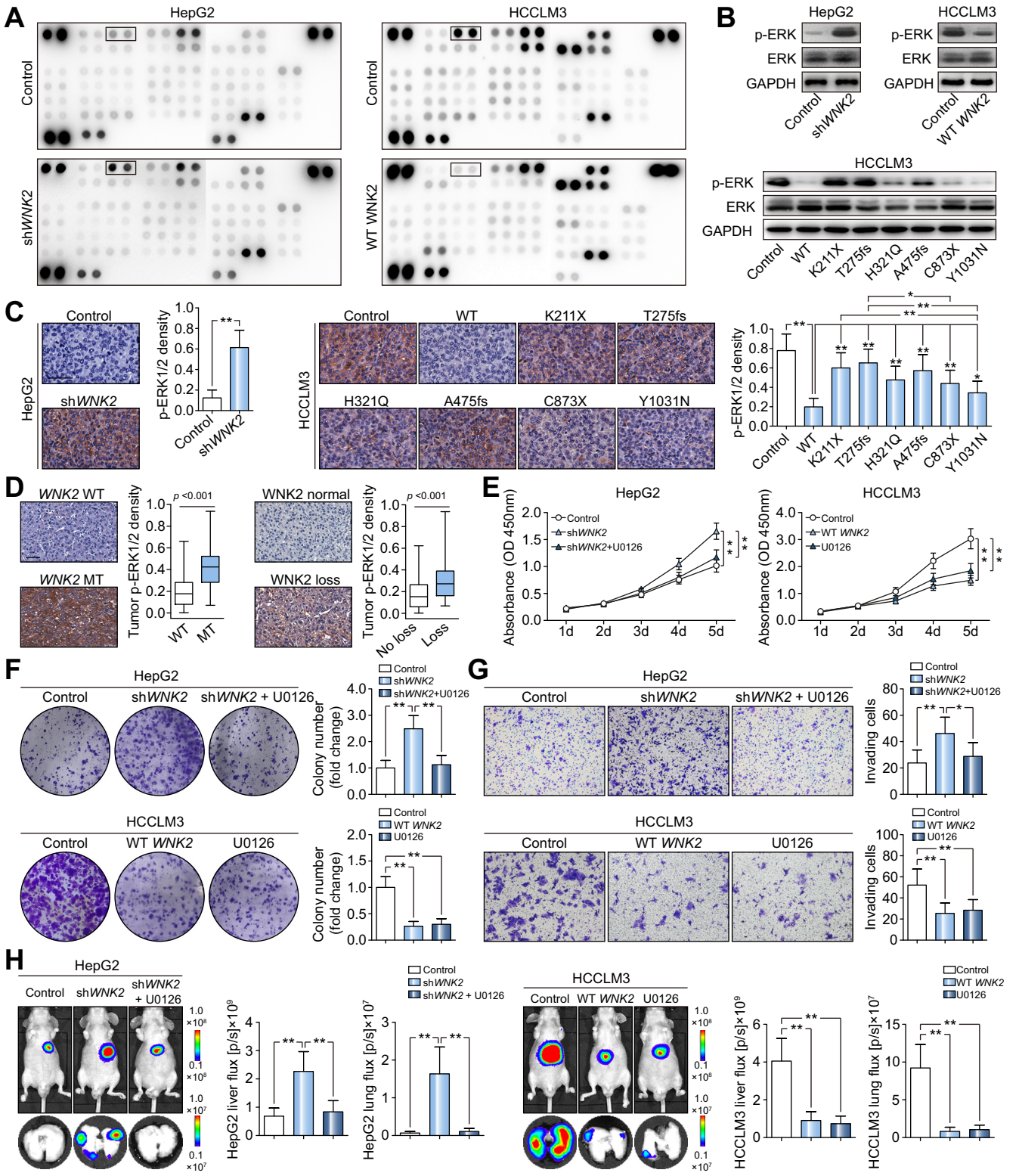

Fig. 5. *WNK2* inactivation leads to ERK1/2 signaling activation in HCC cells. (A) Signaling pathways in HCC cells upon alteration of WNK2 expression screened by probing a human phospho-kinase array. (B) Western blot to validate the expression of p-ERK1/2 in HCC cells upon alteration of WNK2 expression. (C) Representative p-ERK1/2 staining in tumor sections derived from different HCC cell-derived mouse models. The color scale bar depicts the WNK2 staining density in each group, $^{*}p$ <0.05, $^{**}p$ <0.01, student's *t* test was used; scale bars = 50 μm. (D) Representative p-ERK1/2 staining in tumor samples from patients with HCC. The color scale bar depicts the WNK2 staining density, student's *t* test was used; scale bars = 50 μm. (E) Proliferation of U0126-treated HepG2 cells following *WNK2* knockdown and of HCCLM3 cells expressing wild-type *WNK2* or treated with U0126 compared with that of controls, $^{**}p$ <0.01, student's *t* test was used. (F) Colony formation activity of U0126-treated HepG2 cells following *WNK2* knockdown and of HCCLM3 cells expressing wild-type *WNK2* or treated with U0126 compared with that of controls. The bar graphs illustrate the quantification of the colony formation assay, $^{**}p$ <0.01, student's *t* test was used. (G) Cell invasion of U0126-treated HepG2 cells following *WNK2* knockdown and of HCCLM3 cells expressing wild-type *WNK2* or treated with U0126 compared with that of controls. The graphs depict the number of invasive cells after 48 h, $^{*}p$ <0.05, $^{**}p$ <0.01, student's *t* test was used. (H) Representative bioluminescence images of mouse liver tumors and pulmonary metastasis. The color scale bar depicts the photon flux emitted from the mice, $^{**}p$ <0.01, student's *t* test was used.

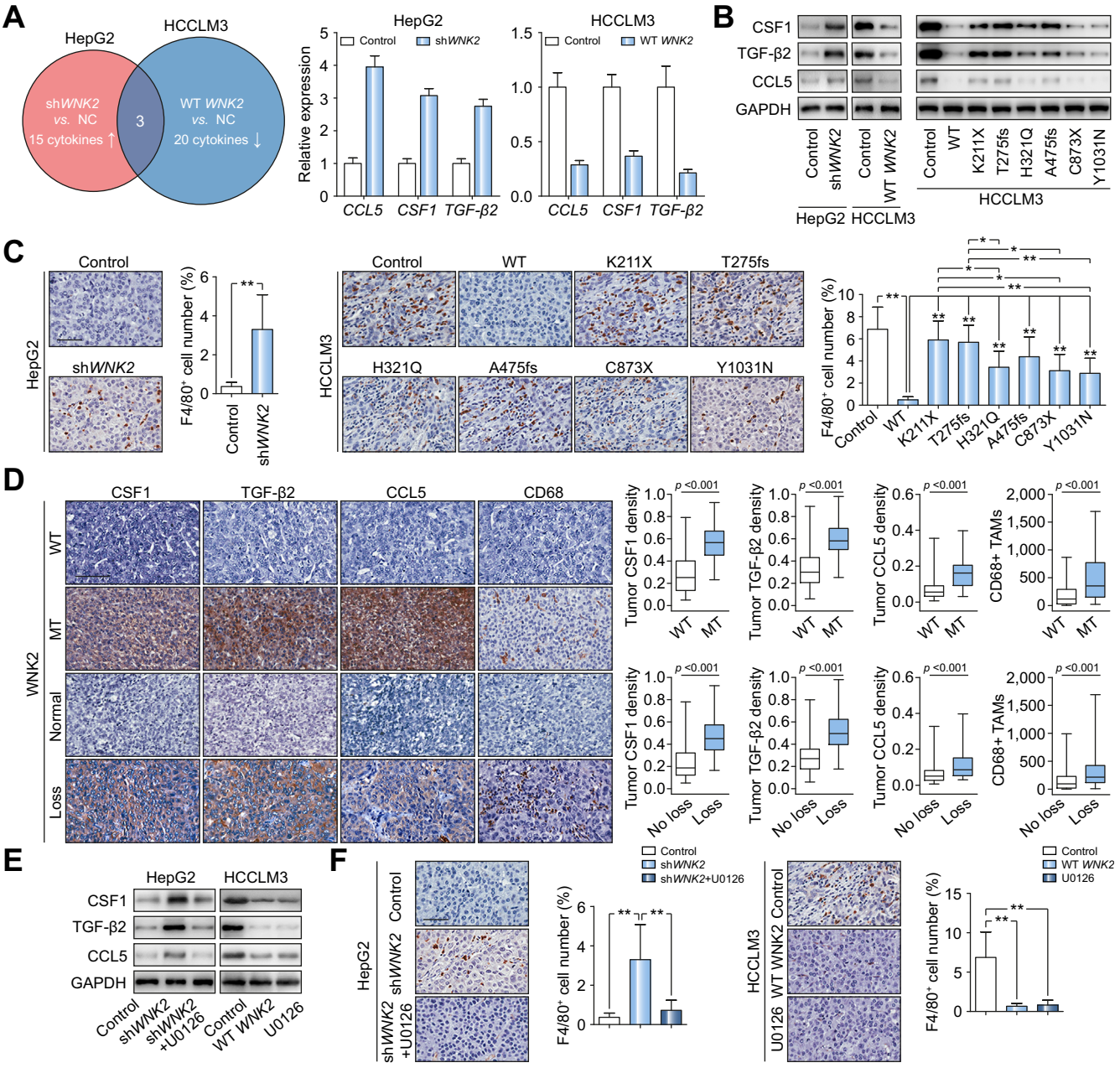

Fig. 6. *WNK2* inactivation promotes tumor-associated macrophage infiltration in mouse models and patients with HCC. (A) Venn diagrams showing the number of cytokines identified that are altered upon WNK2 expression in HCC cells according to 2 groupings: (1) upregulated cytokines in HepG2 cells treated with sh *WNK2*; (2) downregulated cytokines in HCCLM3 cells treated with wild-type *WNK2*. (B) Western blot validated the expression of CSF1, TGFβ2, and CCL5 in parent and stably transfected cells. (C) Representative F4/80 staining in tumor sections derived from different HCC cell-derived mouse models. The color scale bar depicts the F4/80-positive cell number in each group, $^{*}p$ <0.05, $^{**}p$ <0.01, student's *t* test was used; scale bars = 50 μm. (D) Representative CSF1, TGFβ2, CCL5, and CD68 staining in tumor samples from patients with HCC. The color scale bar depicts the staining density and CD68-positive cell number in each group, totaling 736 cases. Student's *t* test was used; scale bars = 50 μm. (E) Western blot showed CSF1, TGFβ2, and CCL5 expression in HepG2 cells and HCCLM3 cells with different treatments. (F) Representative F4/80 staining in tumor sections derived from different HCC cell-derived mouse models. The color scale bar depicts the F4/80-positive cell number in each group, $^{**}p$ <0.01, student's *t* test was used; scale bars = 50 μm.

induced by *WNK2* inactivation in HCCLM3 or HepG2-shRNA-*WNK2* cells, suggesting that *WNK2* inactivation promotes HCC growth and metastasis through ERK1/2 signaling.

WNK2 inactivation promotes tumor-associated macrophage (TAM) infiltration in mouse models and patients with HCC

To further explore the effect of WNK2 on the modulation of the tumor microenvironment, we used PCR arrays to quantify the expression of cytokines and chemokines that were affected by WNK2 expression in HCC cells. We identified 3 cytokines that were upregulated by more than 100% in HepG2 cells after *WNK2* knockdown and downregulated by more than 100% in HCCLM3 cells following *WNK2* overexpression: colony stimulating factor 1 (*CSF1*), C-C motif chemokine ligand 5 (*CCL5*), and transforming growth factor-β2 (*TGFβ2*; Fig. 6A). We validated those results by western blotting (Fig. 6B). Compared with WT *WNK2*, mutated *WNK2* lost its ability to repress those cytokines in HCCLM3 cells (Fig. 6B).

Given that CSF1, CCL5, and TGFβ2 play significant roles in the activation, chemotaxis, and function of macrophages,[21,22] we evaluated the infiltration of TAMs in tumor samples from mouse models and patients with HCC. The numbers of TAMs were significantly increased in HepG2-derived tumors with *WNK2* knockdown. In HCCLM3-derived tumors, overexpression of WT *WNK2* reduced the TAM numbers, while overexpression of mutated *WNK2* failed to suppress TAM infiltration in part or in whole (Fig. 6C). In patients with HCC, those with WT *WNK2* had relatively low levels of CSF1, CCL5, and TGFβ2 expression and had fewer infiltrated TAMs, whereas those with *WNK2* somatic mutations or *WNK2* copy number loss had higher expression levels of those cytokines and more infiltrated TAMs (Fig. 6D). Considering that *WNK2* inactivation leads to ERK1/2 signaling activation in HCC cells, we treated HCCLM3 or HepG2-shRNA-*WNK2* cells with U0126 and observed decreased expression of cytokines/chemokines (Fig. 6E) and reduced numbers of infiltrated TAMs (Fig. 6F), which suggests that *WNK2* inactivation promotes the expression of specific cytokines/chemokines and induces TAM infiltration through ERK1/2 signaling.

Discussion

This study is the most comprehensive description, to date, of the genetic events that characterize Chinese HCCs, which recur early after curative resection. We delineated the genomic landscape, including somatic SNVs/Indels, CNVs, and SVs, in 49 patients with HCC by WGS. Our WGS cohort had a higher mutational burden than other HCC cohorts.[5–7] We propose the following reasons for the relatively high mutational burden in our cohort. First, our WGS cohort was based on patients with HCC who had early tumor recurrence, and higher mutational burden has been associated with poor prognosis in several types of cancer.[23–26] Second, we identified 5 prominent mutational signatures; Signature A (aristolochic acid) and Signature C (aflatoxin) were the dominant signatures in 34.7% (17/49) of the patients, which was different from other HCC cohort studies.[5–7] Exposures to aristolochic acid or aflatoxin are important environmental risk factors for HCC development, especially in China, and are known to contribute to hypermutation in cancer.[3,4] We confirmed that the patients with dominant Signature A or Signature C had a higher mutational burden than the patients without those signatures (Fig. S2C).

Recurrence of HCC after curative resection can be classified as early, occurring within weeks or months, or late, occurring more than 2 years after resection.[27] Early recurrence accounts for nearly 70% of all recurrent HCCs and is attributable to micrometastases that occur in the liver outside of the treated area.[27] In this study, through WGS, WES, and targeted sequencing of 182 HCC samples, we identified mutations in *WNK2, RUNX1T1, CTNNB1, TSC1,* and *TP53* that were correlated with early tumor recurrence after curative resection. The combined mutational profile of those 5 genes showed a strong predictive value and correlated with cumulative recurrence and OS. Although some other genes, such as *TERT*, *AXIN1* and *ARID1A*, have been confirmed as drivers in HCC, they have no ability to predict early HCC recurrence. Our results suggest that *WNK2, RUNX1T1, CTNNB1, TSC1*, and *TP53* may play roles in HCC invasion and metastasis. We also validated the association of *TP53* and *TSC1* mutations with recurrence and OS in an HCC cohort from The Cancer Genome Atlas (TCGA). *WNK2* and *RUNX1T1* mutations showed no ability to predict tumor recurrence or OS, possibly because of their low mutation frequency in the TCGA cohort. In addition, we did not observe any difference in recurrence or OS between patients with a *CTNNB1* mutation and those without a *CTNNB1* mutation. We hypothesize that the difference in the predictive value of *CTNNB1* mutations between our cohort and the TCGA cohort may be caused by differences in racial, etiological, or demographic factors between the cohorts (Fig. S7).

Among the genes that correlated with early tumor recurrence after curative resection, *WNK2* had the most significant difference in mutation frequency and occurred in about 5% of the 736 HCC samples. *WNK2* was mutated in 1.4–3% of HCC samples in other studies from Japan, South Korea, Europe, and the TCGA cohort.[5,6,8,28] In our study of a Chinese HCC cohort, we found that more than half of the *WNK2* mutations were caused by T>A/A>T transversions and C>A/G>T transversions, which are characteristics of Signature A (aristolochic acid) and Signature C (aflatoxin), respectively. We reasoned that this might have contributed to the higher frequency of *WNK2* mutations in our cohort compared with that in other HCC cohorts. Furthermore, in a previous study of 49 aflatoxin-associated HCC samples from the Qidong Liver Cancer Hospital Institute in China, there were somatic *WNK2* mutations in 3 of 49 HCC samples (6.1%), and 2 of those mutations were caused by C>A/G>T transversions, which is a characteristic of Signature C (aflatoxin). That result is consistent with the results of our present study.[3]

WNK2 is a cytoplasmic serine-threonine kinase that belongs to the protein kinase superfamily. WNK kinases play an important role in cell cycle progression, metabolic adaptation, antiapoptosis, invasion, and metastasis.[29] Epigenetic silencing of *WNK2* has been found in gliomas, meningiomas, and pancreatic ductal adenocarcinomas;[30–32] however, the functional impact of genetic mechanisms affecting WNK2 is still unknown, especially in cancer.[29] We showed that in addition to somatic mutations in *WNK2*, copy number loss occurred in nearly 30% of patients, and *WNK2* expression in the tumor samples was also downregulated. Moreover, we demonstrated that *WNK2* somatic mutation, copy number loss, and downregulation were all predictive of early tumor recurrence and shorter OS. Importantly, we revealed through gain-of-function and loss-of-function studies that WNK2 plays a tumor-suppressor role in HCC. We confirmed that *WNK2* inactivation by somatic mutation or downregulation promotes HCC growth and metastasis. Mechanistic study suggested that the effect of *WNK2* inactivation on HCC relies on the ERK1/2 pathway. WNK2 can suppress ERK1/2 signaling in HCC cells, while its inactivation abolishes that suppression. Thus, through clinical and functional study, we demonstrated that *WNK2* is a driver gene in HCC and that its inactivation is predictive of early tumor recurrence and shorter OS.

Different types of non-tumor stromal cells in the surrounding environment can be activated and recruited to the tumor bed.[21,22] Among the stromal cells recruited to the tumor site, macrophages are particularly abundant and are present at all stages of tumor progression.[21] Substantial experimental and clinical evidence suggest that these TAMs promote tumor development and metastasis in the majority of cases.[33] The tumor-promoting functions of TAMs include stimulation of angiogenesis and enhancement of tumor cell proliferation, migration, and invasion,[33] effects that have been recently validated in HCC.[21,34]

Our result showed that *WNK2* inactivation can induce CSF1, CCL5, and TGFβ2 expression through the ERK1/2 pathway and that it also promotes TAM infiltration. Therefore, we hypothesize that WNK2 inactivation promotes HCC not only through a direct effect on ERK1/2 signaling in HCC cells but also by increasing TAM infiltration in the tumor microenvironment.

Taken together, our results delineate the genomic events that characterize Chinese HCCs. We identified *WNK2* as a driver of HCC that was associated with early tumor recurrence after curative resection.

Financial support

This study was jointly supported by the National Key R&D Program of China (No. 2016YFC0902400, 2018YFA0109400), the National Natural Science Foundation of China (No. 81972708; No. 81773069; No. 81830102; No. 81572823; No. 81772578), Shanghai Rising-Star Program (18QA1401200) and Municipal Human Resources Development Program for Outstanding Young Talents in Medical and Health Sciences in Shanghai (2018YQ14).

Conflict of interest

The authors declare no conflicts of interest that pertain to this work.

Please refer to the accompanying ICMJE disclosure forms for further details.

Authors' contributions

SLZ, ZJZ and ZQH performed the experiments; SLZ, CLS and YJL analyzed the data; CBL, HYX, XRY, YHS and ZW provided the samples; SLZ and JZ wrote the paper; XWH, YC and JF commented on the study and revised the paper; JZ obtained funding and designed the research.

Accession codes

All sequencing data were deposited in the Sequence Read Archive (SRA) under accession code number PRJNA504942.

Supplementary data

Supplementary data to this article can be found online at https://doi.org/10.1016/j.jhep.2019.07.014.

References

Author names in bold designate shared co-first authorship

[1] Siegel RL, Miller KD, Jemal A. Cancer statistics, 2017. CA Cancer J Clin 2017;67:7–30.
[2] **Zhou SL**, **Zhou ZJ**, **Hu ZQ**, Huang XW, Wang Z, Chen EB, et al. Tumor-associated neutrophils recruit macrophages and T-regulatory cells to promote progression of hepatocellular carcinoma and resistance to sorafenib. Gastroenterology 2016;150, 1646–1658 e1617.
[3] **Zhang W**, **He H**, **Zang M**, **Wu Q**, **Zhao H**, **Lu LL**, et al. Genetic features of aflatoxin-associated hepatocellular carcinoma. Gastroenterology 2017;153, 249–262 e242.
[4] **Ng AWT**, **Poon SL**, Huang MN, Lim JQ, Boot A, Yu W, et al. Aristolochic acids and their derivatives are widely implicated in liver cancers in Taiwan and throughout Asia. Sci Transl Med 2017:9.
[5] **Totoki Y**, **Tatsuno K**, **Covington KR**, Ueda H, Creighton CJ, Kato M, et al. Trans-ancestry mutational landscape of hepatocellular carcinoma genomes. Nat Genet 2014;46:1267–1273.
[6] **Schulze K**, **Imbeaud S**, **Letouze E**, Alexandrov LB, Calderaro J, Rebouissou S, et al. Exome sequencing of hepatocellular carcinomas identifies new mutational signatures and potential therapeutic targets. Nat Genet 2015;47:505–511.
[7] **Fujimoto A**, **Furuta M**, **Totoki Y**, **Tsunoda T**, **Kato M**, Shiraishi Y, et al. Whole-genome mutational landscape and characterization of noncoding and structural mutations in liver cancer. Nat Genet 2016;48:500–509.
[8] **Ahn SM**, **Jang SJ**, **Shim JH**, **Kim D**, Hong SM, Sung CO, et al. Genomic portrait of resectable hepatocellular carcinomas: implications of RB1 and FGF19 aberrations for patient stratification. Hepatology 2014;60:1972–1982.
[9] **Kan Z**, **Zheng H**, **Liu X**, **Li S**, Barber TD, Gong Z, et al. Whole-genome sequencing identifies recurrent mutations in hepatocellular carcinoma. Genome Res 2013;23:1422–1433.
[10] Nault JC, Zucman-Rossi J. Genetics of hepatocellular carcinoma: the next generation. J Hepatol 2014;60:224–226.
[11] **Bayard Q**, **Meunier L**, **Peneau C**, Renault V, Shinde J, Nault JC, et al. Cyclin A2/E1 activation defines a hepatocellular carcinoma subclass with a rearrangement signature of replication stress. Nat Commun 2018;9:5235.
[12] Tang ZY, Ye SL, Liu YK, Qin LX, Sun HC, Ye QH, et al. A decade's studies on metastasis of hepatocellular carcinoma. J Cancer Res Clin Oncol 2004;130:187–196.
[13] Yang Y, Nagano H, Ota H, Morimoto O, Nakamura M, Wada H, et al. Patterns and clinicopathologic features of extrahepatic recurrence of hepatocellular carcinoma after curative resection. Surgery 2007;141:196–202.
[14] **Zhou SL**, **Dai Z**, **Zhou ZJ**, Wang XY, Yang GH, Wang Z, et al. Overexpression of CXCL5 mediates neutrophil infiltration and indicates poor prognosis for hepatocellular carcinoma. Hepatology 2012;56:2242–2254.
[15] Zucman-Rossi J, Villanueva A, Nault JC, Llovet JM. Genetic Landscape and Biomarkers of Hepatocellular Carcinoma. Gastroenterology 2015;149, 1226–1239 e1224.
[16] **Campbell BB**, **Light N**, Fabrizio D, Zatzman M, Fuligni F, de Borja R, et al. Comprehensive analysis of hypermutation in human cancer. Cell 2017;171, 1042–1056 e1010.
[17] Alexandrov LB, Nik-Zainal S, Wedge DC, Aparicio SA, Behjati S, Biankin AV, et al. Signatures of mutational processes in human cancer. Nature 2013;500:415–421.
[18] Gehring JS, Fischer B, Lawrence M, Huber W. Somatic signatures: inferring mutational signatures from single-nucleotide variants. Bioinformatics 2015;31:3673–3675.
[19] Alexandrov LB, Jones PH, Wedge DC, Sale JE, Campbell PJ, Nik-Zainal S, et al. Clock-like mutational processes in human somatic cells. Nat Genet 2015;47:1402–1407.
[20] **Letouze E**, **Shinde J**, Renault V, Couchy G, Blanc JF, Tubacher E, et al. Mutational signatures reveal the dynamic interplay of risk factors and cellular processes during liver tumorigenesis. Nat Commun 2017;8:1315.
[21] **Mantovani A**, **Marchesi F**, Malesci A, Laghi L, Allavena P. Tumour-associated macrophages as treatment targets in oncology. Nat Rev Clin Oncol 2017;14:399–416.
[22] Krenkel O, Tacke F. Liver macrophages in tissue homeostasis and disease. Nat Rev Immunol 2017;17:306–321.
[23] Owada-Ozaki Y, Muto S, Takagi H, Inoue T, Watanabe Y, Fukuhara M, et al. Prognostic impact of tumor mutation burden in patients with completely resected non-small cell lung cancer: brief report. J Thorac Oncol 2018;13:1217–1221.
[24] **Nava Rodrigues D**, **Rescigno P**, **Liu D**, **Yuan W**, Carreira S, Lambros MB, et al. Immunogenomic analyses associate immunological alterations with mismatch repair defects in prostate cancer. J Clin Invest 2018.
[25] Miller A, Asmann Y, Cattaneo L, Braggio E, Keats J, Auclair D, et al. High somatic mutation and neoantigen burden are correlated with decreased progression-free survival in multiple myeloma. Blood Cancer J 2017;7 e612.
[26] Hwang WL, Wolfson RL, Niemierko A, Marcus KJ, DuBois SG, Haas-Kogan D. Clinical impact of tumor mutational burden in neuroblastoma. J Natl Cancer Inst 2018.
[27] Sherman M. Recurrence of hepatocellular carcinoma. N Engl J Med 2008;359:2045–2047.
[28] Comprehensive and integrative genomic characterization of hepatocellular carcinoma. Cell 2017;169:1327–1341 e1323.

[29] Moniz S, Jordan P. Emerging roles for WNK kinases in cancer. Cell Mol Life Sci 2010;67:1265–1276.
[30] Hong C, Moorefield KS, Jun P, Aldape KD, Kharbanda S, Phillips HS, et al. Epigenome scans and cancer genome sequencing converge on WNK2, a kinase-independent suppressor of cell growth. Proc Natl Acad Sci U S A 2007;104:10974–10979.
[31] **Jun P**, **Hong C**, Lal A, Wong JM, McDermott MW, Bollen AW, et al. Epigenetic silencing of the kinase tumor suppressor WNK2 is tumor-type and tumor-grade specific. Neuro Oncol 2009;11:414–422.
[32] Dutruel C, Bergmann F, Rooman I, Zucknick M, Weichenhan D, Geiselhart L, et al. Early epigenetic downregulation of WNK2 kinase during pancreatic ductal adenocarcinoma development. Oncogene 2014;33:3401–3410.
[33] Noy R, Pollard JW. Tumor-associated macrophages: from mechanisms to therapy. Immunity 2014;41:49–61.
[34] **Zhou SL**, **Hu ZQ**, **Zhou ZJ**, Dai Z, Wang Z, Cao Y, et al. miR-28-5p-IL-34-macrophage feedback loop modulates hepatocellular carcinoma metastasis. Hepatology 2016;63:1560–1575.